

# Galerkin finite volume solution of heat generation and transfer in RCC dams

S.R. Sabbagh-Yazdi, N.E. Mastorakis, and A.R. Bagheri

**Abstract**—Galerkin Finite Volume solution of the temperature field on unstructured finite volumes is introduced. In this software, the transient PDE for heat transfer in solid media is coupled to a suitable concrete heat generation algebraic relation. The discrete form of the heat transfer equations is derived by multiplying the governing equation by a piece wise linear test function and integrating over a sub-domain around any computational node. The solution domain is divided into hybrid structured/unstructured triangular elements. The triangular elements in the structured part of the mesh can be activated for simulating gradual movement of the top boundary domain due to advancing the concrete lifts. The accuracy of the developed model is assessed by comparison of the results with available analytical solutions and experimental measurements of two-dimensional heat generation and transfer in a square domain. Then, the computer model is utilized to simulate the transient temperature field in a typical RCC dam section.

**Keywords**—Heat Generation and Transfer, NASIR Finite Volume Solution, RCC Dam Construction Program

## I. INTRODUCTION

In the mass concrete structures such as Compacted Concrete Roller (RCC) dams the heat generation due to cement hydration and the heat exchange with the surrounding ambient result in time varying temperature profiles in the structure. Tensile stresses develop in the structure due to restrained thermal movements. Leaving unchecked such an effect can result in thermal cracking of the concrete. The use of RCC method and fast construction of thin layers makes major difficulties for the application of post cooling techniques. Since, the layered based mass concrete, which is used in the core body of the RCC dams, can considerably speed up the procedure of the construction, thermal considerations are critical tasks in such a massive concrete structure. Therefore, prediction of temperature profiles has been an important part of the design and construction process.

The heat exchange in RCC dams principally takes place in the transverse direction of the dam axis. Therefore, two-

dimensional models are generally adopted for temperature studies [1,2]. The temperature analysis of a concrete structure is associated with temperature dependent heat sources of cement hydrations all over the domain. However, the heat generation rate of the cement contents with gradually increasing section, depends on the temperature of surrounding concrete and the heat conduction properties of the aggregates, the computation of the temperature profiles is not an easy task.

In this paper, first the mathematical model of the phenomena including the transient partial differential equation of heat transfer and associating boundary conditions in conjunction with an algebraic formula for the source term of the heat generation rate is described. Then, the numerical techniques employed for deriving the algebraic formula suitable for numerical solution on a triangular mesh is discussed. For the present solution algorithm, the domain discretization technique using hybrid unstructured/structured triangular mesh, taking into account the layer-based movement of the top surface boundary of the concrete structure is introduced. The accuracy of the solution of the spatial derivative part of the governing equation is verified using the analytical solution of heat transfer in a square domain. Then, the quality of the formula adopted for the source term of cement heat generation rate is assessed by the use of available experimental measurements on a concrete block. Finally, the developed model is applied for prediction of the transient temperature field in a typical RCC dam section during the construction and after the completion. For this case, the abilities of the developed model to investigate the effects of variation in amount of cement per cubic meter, layer thickness and time lag between placing two consequent layer of concrete are demonstrated.

## II. GOVERNING EQUATION

Since heat exchange in many massive structures such as RCC dams, retaining walls and tunnel linings principally takes place in the transverse direction of the long axis, two-dimensional models are generally adopted for temperature studies. Assuming isotropic thermal properties for the solid materials, the familiar two-dimensional equation defining heat generation and transfer is of the form,

$$\alpha \nabla^2 T + \frac{\alpha}{\kappa} \dot{Q} = \dot{T} \quad (1)$$

Manuscript received May 1, 2007; Revised received October 12, 2007

Saeed-Reza Sabbagh-Yazdi is Associate Professor Civil Engineering Department of K.N. Toosi University of Technology, 1346 Valiasr St. Tehran, IRAN (phone: +9821-88521-644; fax: +9821-8877-9476; e-mail: SYazdi@kntu.ac.ir).

Nikos E. Mastorakis, is Professor of Military Institutes of University Education (ASEI) Hellenic Naval Academy, Terma Chatzikyriakou 18539, Piraeus, GREECE. Nikos Mastorakis is also with the WSEAS.

Ali-Reza Bagheri is Assistant Profesor of Civil Engineering Department of K.N. Toosi University of Technology, 1346 Valiasr St. Tehran, IRAN

where, the parameters are  $T(^{\circ}C)$  temperature,  $K (W/m^{\circ}c)$  heat conduction coefficient and  $\dot{Q} (KJ/m^3h)$  rate of heat generation per unit volume and the thermal diffusion is defined as  $\alpha = \kappa / \rho C$  with  $\rho (Kg/m^3)$  being the density and  $C (KJ/Kg^{\circ}c)$  the specific heat of concrete. The parameter  $\dot{Q}$ , which acts as a source term, is the rate of heat generation due to cement hydration in the concrete field.

The natural boundary condition on concrete external surface is taken as,

$$\kappa(\nabla T \cdot \hat{n}) + q = 0 \tag{2}$$

where,  $q$  is the rate of heat exchange per unit volume of concrete surface with surrounding ambient and  $\hat{n}$  is the unit vector normal to the boundary surface. The rate of heat exchange  $q$  is taken into consideration through three mechanisms,  $q_c$  (convection),  $q_r$  (long wave radiation of concrete to surroundings) and  $q_s$  (solar radiation absorption). Hence, the total rate of heat exchange can be defined as,  $q = \pm q_c + q_r - q_s$  [1,2].

Note that,  $q_c$  is through air (or water) movement and depends on the difference between temperature of the concrete surface,  $T_s$ , with surrounding ambient temperature,  $T_{air}$ , and is given by  $q_c = h_c (T_s - T_{air})$ . Where,  $h_c = h_n + h_f$  is coefficient of thermal convection comprising from the natural convection coefficient,  $h_n = 6 \left( W/m^2^{\circ}C \right)$ , and forced convection coefficient,  $h_f = 3.7V$ , where  $V(m/s)$  is the wind speed.

It is worth noting that, if insulation (form work) is applied on the concrete surface, the modified coefficient of thermal convection may be determined using following algebraic formula  $h'_c = \left[ 1/h_c + (e/\lambda)_{Insulation} \right]^{-1}$ ,  $(KJ/m^2h^{\circ}C)$ . Where,  $e$  and  $\lambda$  are the form insulation thickness and its coefficient of thermal convection, respectively.

For long wave radiation a similar relationship is used as  $q_r = h_r (T_s - T_{air})$ . Where,  $h_r$  is the coefficient of thermal radiation.

Short wave exchange rate  $q_s$  is given by  $q_s = \alpha I_n$ . Where  $\alpha$  is surface absorption coefficient and the parameter  $I_n$  is incident normal solar radiation.

One of the main factors influencing temperature profiles in concrete sections is the amount and rate of heat generated by the cementitious materials present in the concrete [3]. Due to the considerable influence of concrete temperature on the hydration rate of cementation materials, it is necessary to take this effect into account in the simulation method [1,4,5].

The effect of temperature history of each point on its rate of heat generation was taken into account in this research by the concepts of maturity functions  $f(t)$  and equivalent time,  $t_e$ . Maturity functions define the temperature dependence of

cement hydration reactions. Two commonly used such functions are named after Rastrup [2] and Arrhenius [1,5] and are given as:

$$f(T) = k 2^{\left(\frac{T}{10}\right)} \quad (\text{Rastrup}) \tag{3}$$

$$f(t) = k \exp \left\{ \frac{-E}{R(273+T)} \right\} \quad (\text{Arrhenius}) \tag{4}$$

$K$  = Constant factor

$T$  = Concrete temperature in  $^{\circ}C$

$E$  = Activation Energy  $(J/mol)$

$E = 33500$  for  $T \geq 20^{\circ}C$

$E = 33500 + 1470(20 - T)$  for  $T < 20^{\circ}C$

$R$  = Molar gas constant =  $8.314 J/^{\circ}C mol$

As seen above, an increase in concrete temperature,  $T$ , results in an increase in the maturity function,  $f(t)$ . Using such functions, the relative speed of reaction at any temperature,  $T$ , in comparison with that at a reference temperature,  $T_r$ , can be obtained. The relative speeds of reaction,  $H(T)$ , based on Rastrup and Arrhenius functions are derived as

$$H(T) = 2^{0.1(T-T_r)} \quad (\text{Rastrup}) \tag{5}$$

$$H(T) = \exp \left\{ \frac{E}{R} \left( \frac{1}{273+T_r} - \frac{1}{273+T} \right) \right\} \quad (\text{Arrhenius}) \tag{6}$$

Having obtained the relative speed of reaction at various temperatures to that at a reference temperature  $T_r$ , the equivalent time ( $t_e$ ) at this reference temperature for each point in concrete with its particular temperature profile  $T(t)$ , can be calculated:

$$t_e = \int H(T) dt \tag{7}$$

By obtaining the equivalent time,  $t_e$ , for each point in concrete, its rate of heat generation can be derived from the base heat generation curve of the concrete under a reference temperature,  $T_r$ . The basic heat generation curve is generally derived for the concrete mix under study by experimental determination.

In this work, suitable functions are fitted to the experimental data and the heat generation function  $Q(t_e)$  is obtained. Different concretes have different heat generation characteristics. Therefore, there have been a number of functions proposed for defining this parameter.

Two of the common ones are proposed by Rastrup [2] and Gofredson [5]:

$$Q(t_e) = A + E \exp\{-b[t_e]^n\} \quad \text{(Rastrup)} \quad (8)$$

$$Q(t_e) = A(1 - e^{-\frac{t_e}{B}}) \quad \text{(Gotfredson)} \quad (2.9)$$

where,  $A, E, B$  and  $b$  are constants determined by regression analysis of experimental results.

In the developed software, the user has the option of choosing either of the two maturity functions. Also either of the two proposed basic heat generation functions can be chosen. Any other maturity or heat generation function required can also be easily programmed into the software.

Based on the derivations given above the rate of heat generation for any point in concrete can now be determined at any equivalent time,  $t_e$ , using the following procedure:

$$\dot{Q}(t_e) = \left( \frac{dQ(t_e)}{d(t_e)} \right) \left( \frac{d(t_e)}{dt} \right) \quad (10)$$

Remember that from equation (2.7) we have,

$$\frac{d(t_e)}{dt} = H(t) \quad (11)$$

Choosing Rastrups relative rate of reaction for  $H(T)$ , i.e: equation (2.5) we get:

$$\frac{d(t_e)}{dt} = 2^{0.1(T-T_r)} \quad (12)$$

For the term  $dQ(t_e)/d(t_e)$ , if we choose Rastrups function for basic heat generation curve  $Q(t_e)$  (ie, equation (2.8)), we will get:

$$\frac{dQ(t_e)}{d(t_e)} = nbE \{(t_e)^{-n-1} \exp[-b(t_e)^{-n}]\} \quad (13)$$

Combining equation (2.12) and (2.13) for obtaining  $\dot{Q}(t_e)$  we have:

$$\dot{Q}(t_e) = nbE (t_e)^{-n-1} \exp\{-b(t_e)^{-n}\} 2^{0.1(T-T_r)} \quad (14)$$

However, the program enables the user to choose any other combination of maturity function and basic heat generation functions for the derivation of  $\dot{Q}(t_e)$ .

### III. FINITE VOLUME FORMULATION

Here, a fast and accurate numerical technique is introduced which efficiently enables solution of the temperature field in two-dimensional domains with complex and moving boundaries by the use of mixed structured/unstructured triangular meshes [9].

In order to convert the governing partial differential equation into the discrete for Galerkin Finite Volume Method

is used. For this propose, first the governing equation for heat generation and transfer is written in the following two-dimensional form,

$$\frac{\partial T}{\partial t} + \frac{\partial F_i^T}{\partial x_i} = S \quad (i=1,2) \quad (15)$$

where  $T$  (temperature) is the unknown parameter and  $S_n$  is the heat source, and temperature flux in  $i$  direction is defined as  $F_i^T = \alpha \frac{\partial T}{\partial x_i}$ .

The governing equation is multiplied by a piece wise linear test function on triangular element meshes, and then, it is integrated over all triangles surrounded every computational nodes (vertices of the triangular elements). By application of Gauss divergence theorem and using the property of the test function, which satisfies homogeneous boundary condition on the dependent variable, the boundary integral terms can be omitted. After some manipulations, the resulted equation can be written as,

$$\int_{\Omega} \left( \frac{\partial T_n}{\partial t} \right) \phi d\Omega = \int_{\Omega} (F_i^d \frac{\partial \phi}{\partial x_i})_n d\Omega + \int_{\Omega} S_n \phi d\Omega \quad (i=1,2) \quad (16)$$

The procedure of deriving algebraic equation will end up with an efficient explicit numerical algorithm by using of following formula within each sub-domain  $\Omega$  consisting the triangles associated with every node  $n$  [9],

$$T_n^{t+\Delta t} = T_n^t + \Delta t \left[ S_n - \frac{3}{2\Omega_n} \left( \sum_{k=1}^N F_i^d \Delta l_i \right)_n \right] \quad (i=1,2) \quad (17)$$

where,  $\Delta l_i$  is the  $i$  direction component of normal vector of  $m^{\text{th}}$  edge of each triangle. The area of sub-domain,  $\Omega$  can be computed by summation of the area of the triangles  $\Lambda$  associated with node  $n$ , using

$$\Lambda = \int_{\Lambda} x_i (d\Lambda)_i \approx \sum_k^3 [\bar{x}_i \delta \ell_i]_k$$

Note that, using the linear interpolation function for the temperature, the algorithm takes advantage from the fact that the first derivatives of  $F_i^T$  are constant inside each triangular element. By application of the Gauss divergence theorem, the piece wise constant temperature flux in  $i$  direction,  $F_i^d$ , at each triangular element can be calculated using following algebraic formula,

$$F_i^d = \frac{1}{\Lambda} \sum_{m=1}^3 (\bar{T} \Delta l_i)_m \quad (18)$$

where,  $\bar{T}$  is the average temperature of the edge. The resulting discrete formulation can be solved explicitly with rather light computational efforts.

Using meshes with various sub-domain sizes of sub-domains, to maintain the stability of the explicit time stepping the minimum time step of the domain of interest should be as,

$$\Delta t = k \left( \frac{\Omega_n}{\alpha_n} \right)_{\min} \quad (19)$$

Remember, the heat source for each node  $n$  in concrete body is defined by  $S_n = \alpha_n \dot{Q}(t_e)_n / \kappa_n$ .

If  $a$  and  $\kappa$  at node  $n$  are considered independent of time and temperature and maturity of the concrete, then for determination of the heat source in every time step, only the value of heat generation rate  $\dot{Q}(t_e)$  at nodes located in concrete body must be updated for the nodes using equation (2.3). It should be noted that the value of  $\dot{Q}(t_e)$  in each node is a function of  $t_e$  for that node. Therefore,  $t_e$  should be updated at each time step using following formula,

$$t_e = \sum_{t=t_0}^{t=t_0+N\Delta t} (2^{0.1(T-T_c)}) \Delta t \quad (20)$$

Two types of boundary conditions are usually applied in this numerical modeling. The essential and natural boundary conditions are used for temperature at boundary nodes and temperature diffusive flux (gradients) at boundary elements, respectively [10-12].

For the boundaries where the natural boundary conditions are to be applied, by the use of equation (2.2) (the temperature gradient normal to the surface boundary proportional to  $q$ ) and the temperature at the nodes at the vicinity of the boundary, the temperature at boundary nodes can be computed and imposed.

#### IV. GEOMETRY MODELING

The solution comprises of the concrete dam body and the foundation. Considering the regular geometry of dam cross section and in order to facilitate the movement of the upper boundary of concrete as layered sequences of construction progresses, the use of structured mesh [13] is considered for dam body. Numbering the nodes and elements from the base layer to the top layer of the dam, provides the ability to ignore the desired upper layers of the dam.

For construction of structured part of the mesh, the nodal points are defined by intersection of series of columns and rows. Then by the use of inclined lines each area within the four nodes is divided into two triangles. In this type of mesh the required shape of upstream and downstream boundaries of a dam can easily be taken into account. Since the age of concrete varies from layer to layer in the body of RCC dam, the use of regular mesh spacing allows moving the top boundary by gradual increasing the number of layers with constant thickness. The structured mesh is therefore quite appropriate because of offering control on the layer thickness and sequence of construction.

The dam foundation, where moving boundary is not required, is discretized using unstructured mesh. This will facilitate consideration of foundations irregularities (various materials properties at different zones). The irregular

triangular mesh was produced using Deluaney Triangulation technique [13]. Such a mesh generation method allows local refinement of triangular elements by using source points and lines. In this type of mesh the address of each node (coordinates) plus the three nodes making up each triangle are explicitly defined. The use of unstructured mesh for the foundation of the dam has the advantage of allowing finer mesh size near high heat temperature gradient zones (i.e. the dam body). This technique increases the speed and accuracy of the computations (Figure 1).

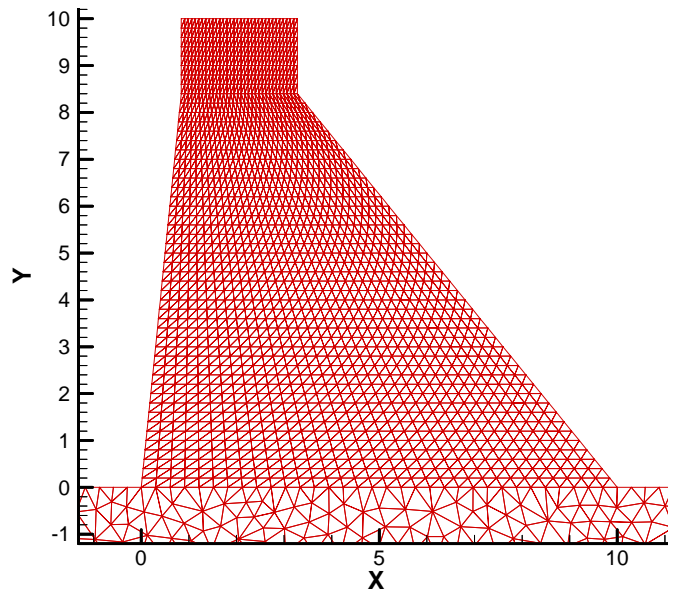


Fig. 1. Hybrid structured/unstructured triangular mesh of dam and foundation

#### V. MODEL VERIFICATION

In order to evaluate the accuracy of the source term representing the rate of the heat generation, a set of experimental measurements on a concrete cube with 60 (cm) dimensions cast by 450 kilogram per cubic meter is used. The concrete block was insulated all over the faces. The properties of concrete is considered as  $\alpha_c = 0.0038 \text{ (m}^2/\text{h)}$  and  $\kappa = 9 \text{ (KJ/m}^2\text{ch)}$ . The averages of measured temperature at three points of this concrete block (one point at the center and two points near the faces) reported by previous workers [7].

A two dimensional rectangular triangular mesh with 6 (cm) spacing is utilized for numerical simulations of this case. The results of the computer model with the 13.5°C concrete placing temperature present reasonable agreements with the experimental data for the permanently isolated concrete block (Figure 2).

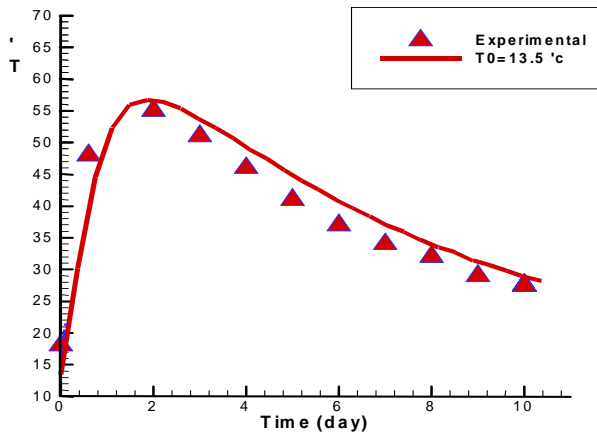


Fig. 2. Comparison of computed results ( $T_0=13.5\text{ }^\circ\text{C}$ ) with the experimental data

At the next stage, the accuracy of the solution of spatial derivative terms is investigated by comparison of the results of the numerical solver with the analytical solution of the following two-dimensional boundary value problem with a constant source term as,

$$\frac{\partial^2 T}{\partial x_i^2} = 1 \quad \Omega = \{0 < (x_1, x_2) < 1\} \quad (21)$$

The boundary conditions are considered  $T = 0$  at  $x_1 = 1$ ,  $x_2 = 1$  and  $\frac{\partial T}{\partial n} = 0$  at  $x_1 = 0$ ,  $x_2 = 0$ . The analytical solution is given by [11],

The numerical modeling of the case is performed on  $20 \times 20$  grid for triangular meshing. The computed temperature profiles on the utilized triangular mesh are plotted in figure 3. In Figure 4, the results of numerical computations are compared with the analytical solution of the case [14].

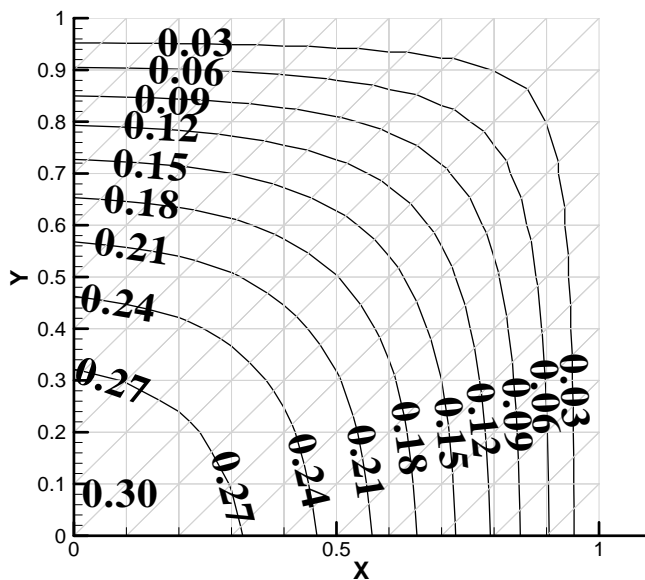


Fig. 3. Computed temperature contour map in the up standing square field

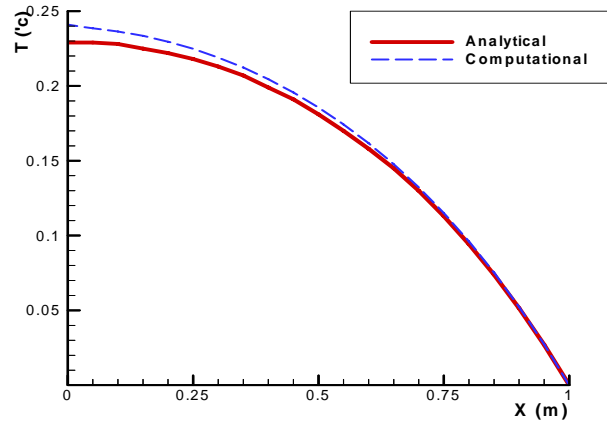


Fig. 4. Comparison of computed and analytical results on the  $y = 30\text{ cm}$

### VI. APPLICATION OF THE MODEL

In order to present the ability of the model to deal with real world cases, it is applied to a typical gravity dam section. Both the base and the height of the section are considered as 10 (m) while the dam crest width is considered as 2.5 (m). Upstream and downstream slopes are designed as 0.1:1.0 and 0.8:1.0, respectively. The radius of the half circle shape far field boundary was considered 1.5 times of the dam base dimension [14].

The regular mesh of the RCC dam body is generated with 0.2 (m) vertical spacing. The horizontal spacing at the dam base is

$$T(x_1, x_2) = \frac{1}{2} \{ (1 - x_2^2) \} + \frac{32}{\pi^3} \sum_{n=1}^{\infty} \frac{(-1)^n \cos \left[ (2n-1)\pi x_2 / 2 \right] \cosh \left[ (2n-1)\pi x_1 / 2 \right]}{(2n-1)^3 \cosh (2n-1)\pi / 2} \quad (22)$$

considered equal to 0.3 (m) and reduced in upper layers proportional to the dam width. The horizontal mesh spacing at the dam base was taken as the finest part of the unstructured triangular mesh of the foundation part of the domain, and the triangles sizes increase far from the dam base center.

Following assumptions were made for concrete placing program. The layers are constructed every 24 hours at the thickness of 0.4 (m). The cement content of the concrete is 150 ( $\text{kg}/\text{m}^3$ ). The concrete placing temperature is considered 25  $^\circ\text{C}$ . The ambient temperature variation is assumed to vary between 20 and 30  $^\circ\text{C}$ . Considered no isolations at dam wall, severe conditions are provided for the numerical computations due to high temperature gradients at boundaries of the solution domain. The properties of RRC dam is considered as  $\alpha = 0.0038$  ( $\text{m}^2/\text{h}$ ) and  $\kappa = 9$  ( $\text{KJ}/\text{m}^\circ\text{c h}$ ). Rock foundation is considered to be quartzite with material properties of  $\alpha = 0.009$  ( $\text{m}^2/\text{h}$ ) and  $\kappa = 6$  ( $\text{KJ}/\text{m}^\circ\text{c h}$ ).

The results of the computational model for some of the stages of layer-based construction of a 10 (m) height RCC

dam are shown in the form of temperature contour maps (Figure 5).

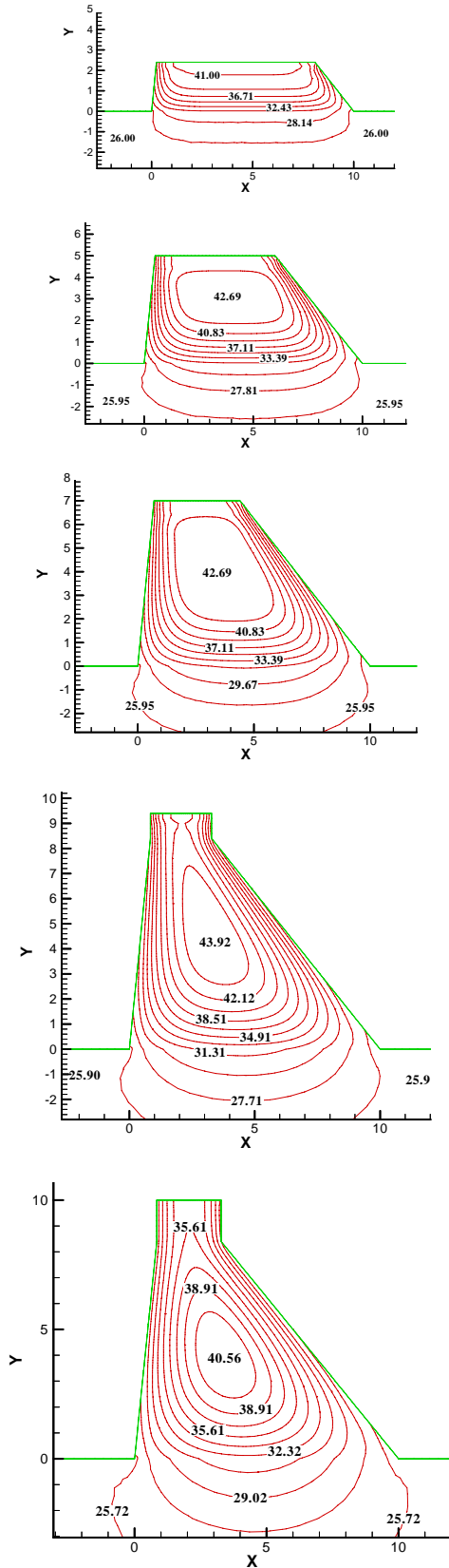


Fig. 5. Temperature field at four stages of layered concrete placing of a 10 m height RCC dam without form works during construction

Figure 6 presents the computed temperature history (at center of the dam width) of four points at the levels 2, 4, 6 and 8 (m) from the base, starting from their concrete placing time in the computational domain.

Figure 7 presents the comparison between average and maximum temperature of the field as the dam section rises. As can be seen in the figure 7, the maximum temperature of the central points located at 2, 4 and 6 (m) above the dam base coincide with the maximum temperature of the domain. The maximum temperature at central point 8 (m) above dam base, which is near the dam crest (where the width of the section is narrow), is less than maximum temperature of the field. This shows that, by considering above mentioned design and program for the construction, during the final stages of the dam construction, the maximum temperature will occur somewhere else rather than the newly placed concrete layers (i.e. at the core of the section). This is in general agreement with the observed temperature fields of real RCC structures.

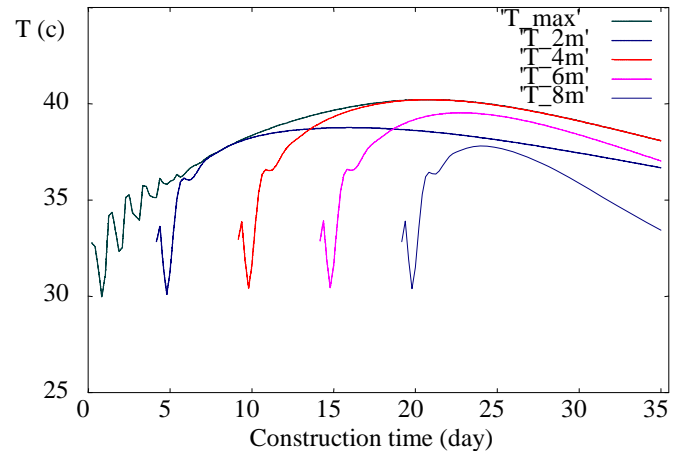


Fig.6. The computed temperature history of four points

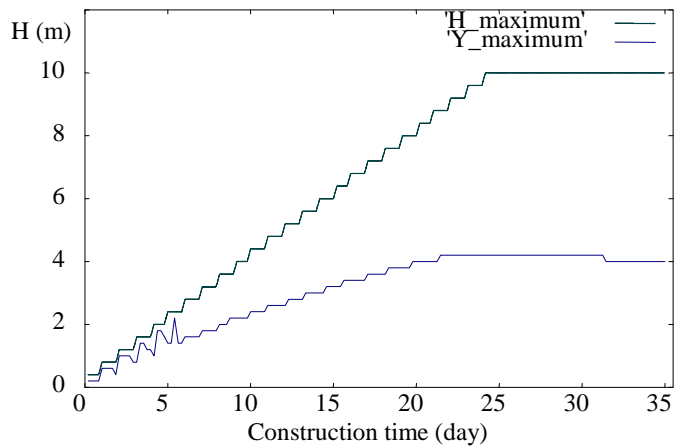


Fig.7. The maximum temperature of the domain.

The developed model is applied for prediction of the effects of various factors in concrete placing. For this purpose, the above typical RCC dam is utilized.

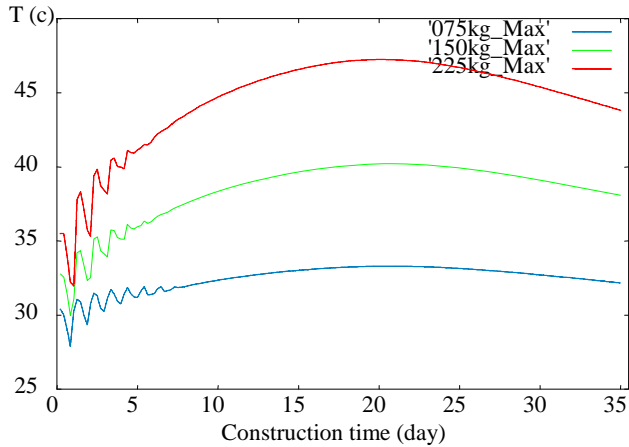


Fig. 8. The history of maximum temperature for three different amounts cement concrete

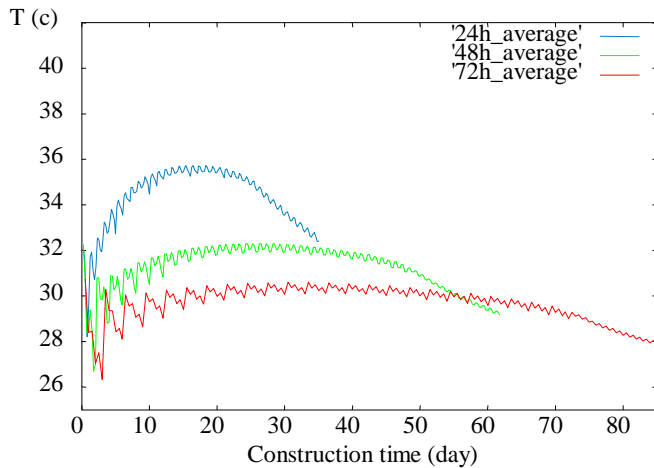


Fig.9. The effects of time lag between concrete placing on average temperature of the section during the construction time

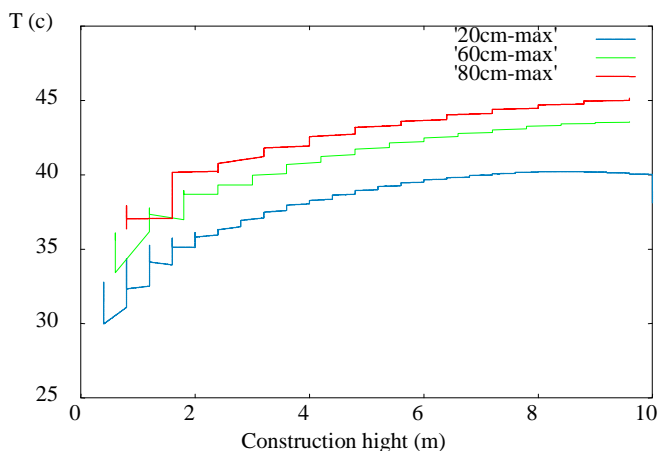


Fig.10. The increase of maximum temperature due to use of various thickness of concrete layers

The history of maximum temperature for three different amounts 75, 150 and 225 ( $kg/m^3$ ) cement concrete in concrete are compared at figure 8. The obvious direct effect of amount of cement contents on the maximum temperature of the domain is correctly simulated by the developed numerical solver.

In figure 9, the worse effects of time lag between concrete placing is presented by comparing the nonlinear differences of three time lag of 24, 48 and 72 hours between concrete placing of sequential layers.

The increase of maximum temperature due to use of thick concrete layers are demonstrated in figure 10. As can be seen, the maximum temperature varies linearly with the amount of cement content in the concrete setting.

## VII. CONCLUSION

In this paper Galerkin finite volume method which is adapted for solution of the heat transfer equation considering the heat generation rate (due to cement hydration) is described. The governing equation is discretized on hybrid structured-unstructured mesh of triangular element. The resulted algorithm provides light explicit computation of time dependent problems. The simplicity of the algorithm makes it easy to program and extension for further developments.

The numerical model was verified in two stages. Firstly, the adopted formulation for the term representing heat generation rate of the concrete is evaluated by the comparison of the computed results with the available experimental measurements on a concrete block. Secondly, the accuracy of the solution of the heat transfer terms was assessed using a boundary value problem and its analytical solution. The results of the developed model present reasonable agreements to the analytical solution and experimental measurements.

By application of structured mesh for the concrete dam part of the domain, an efficient modeling of the layered based construction of concrete structures (RCC Dam) is achieved. Gradual movement of the top boundary of the structure during the construction period is simulated by deactivating the upper part of the dam, in which no concrete is placed. For discretization of the dam foundation, unstructured mesh of triangles is considered, which facilitates considering irregularities in geometrical features and material properties of the natural foundation. The developed model was applied to a typical RCC dam section and the results of the temperature fields obtained showed the general pattern expected for such structures.

The developed matrix free Galerkin finite volume heat generation and transfer solver can serve as a tool for analyzing the effects of changes in cement content in the concrete mixture, thickness of the concrete placing layers and time lag between placing two sequential concrete layers setting. Therefore, it can be used for forecasting time dependent temperature profiles due to desired design and construction program of layered base mass concrete structures such as RCC dams as well as the modification and optimization of the design and construction program.

## REFERENCES

- [1] S. B. Tatro, E. K. Shrade, *Thermal analysis for RCC, a practical approach*, Proceeding of the Conference on Roller Compacted Concrete A.S.C.E., New York, 1992.
- [2] K. D. Hansen, W. G. Reinhardt, *Roller compacted concrete dams*, Mac Grow Hill Company, New York, 1991.
- [3] H. H. Gotfredson, G. M. Idorn, Curing technology at the force Bridge Denmark. ACI S.P. 95, 1986, pp17-33.
- [4] A. R. Bagheri, *Early age thermal effects in conventional and micro-silica concrete linings*. PhD Thesis, University of Newcastle, UK, 1990.
- [5] E. L. Wilson, *Determination of temperatures within mass concrete structure*, Report No. 68-17, Department of Civil Eng., University of California, Berkeley, 1968.
- [6] M. Lachemi, P. C. Aitcin, *Influence of ambient and fresh concrete temperatures on maximum temperature and thermal gradient in a high performance concrete*, ACI Materials Journal, 1997, pp 102-110.
- [7] F. A. Branco, P. A. Mendes, E. Mirambell, *Heat of hydration effects in concrete structures*. ACI Materials Journal, 1992, pp 139-145.
- [8] L. A. Sykes, *Development of a two-dimensional navier-stokes algorithm for unstructured triangular grids*. ARA Report 80, 1990.
- [9] S. R. Sabbagh Yazdi, A. R. Bagheri, *Computer Simulation of Cement Heat Generation and Temperature Profiles in Mass Concrete Structures*, International Journal of Engineering Science, Vol. 15, No2, 2004, pp65-71.
- [10] S. V. Patankar, *Numerical heat transfer and fluid flow*. McGraw Hill, 1980.
- [11] J. N. Reddy, *An introduction to the Finite Element Method*, McGraw-Hill, Mathematics and Statistics Series, 1984.
- [12] D. A. Anderson, J. C. Tannehill, R. H. Pletcher, *Computational fluid mechanic and heat transfer*. Combridge Hemispher Press, 1984.
- [13] J. F. Thompson, B. K. Soni, N. P. Weatherill, *Hand book of grid generation*, CRC Press, 1999.
- [14] V. Salehi-Goorabsari, *Two dimensional numerical modeling of heat generation and transfer in mass concrete using triangular meshes*. MSc Thesis, Faculty of Civil Engineering, KNToosi University of Technology, Iran, 2002.

First Author's biography may be found in following site:

<http://sahand.kntu.ac.ir/~syazdi/>